Direct Solar Viewing Calibration Concept for Future CERES-, GERB-, or Libera-Type Earth Orbital Climate Missions

G. MATTHEWS[a]

[a] *Zedika Solutions LLC, Fort Wayne, Indiana*

(Manuscript received 10 February 2021, in final form 19 March 2022)

ABSTRACT: Better predictions of global warming can be enabled by tuning legacy and current computer simulations to Earth radiation budget (ERB) measurements. Since the 1970s, such orbital results exist, and the next-generation instruments such as one called "Libera" are in production. Climate communities have requested that new ERB observing system missions like these have calibration accuracy obtaining significantly improved calibration SI traceability and stability. This is to prevent untracked instrument calibration drifts that could lead to false conclusions on climate change. Based on experience from previous ERB missions, the alternative concept presented here utilizes directly viewing solar calibration, for cloud-size Earth measurement resolution at <1% accuracy. However, it neglects complex already used calibration technology like solar diffusers and onboard lights, allowing new lower cost/risk unconsidered spectral characterizing concepts to be introduced for today's technology. Also in contrast to near future ERB concepts already being produced, this enables in-flight wavelength dependent calibration of Earth-observing telescopes using direct solar views, through narrowband filters continuously characterized on-orbit.

KEYWORDS: Climate records; Instrumentation/sensors; Measurements; Remote sensing; Satellite observations

1. Introduction

It is vital to both continue and significantly improve accuracy of orbital Earth radiation budget (ERB) shortwave (SW; 0–5 μm) and longwave (LW; 5–200 μm) measurements of fluxes leaving Earth at the top of the atmosphere (TOA). In the field of climate model validation, this gives confidence in global warming computer predictions, if their legacy and legacy and current simulations match ERB measurements at the same time and locations, etc.

By far the most extensive ERB SW results come from a NASA mission called the Clouds and the Earth's Radiant Energy System (CERES; Wielicki et al. 1996), with six instruments covering the globe, providing a continuous climate measurement record since 2000. These measure from sun-synchronous U.S. polar-orbiting satellites, called *Terra* (March 2000→) and *Aqua* (July 2002→; see NASA 2021). Such data are supplemented by those from the European Geostationary Earth Radiation Budget (GERB; Harries et al. 2005) mission, which provides 15-min time resolution from its higher orbit viewing Africa/Europe. CERES results, however, are known to have insufficient accuracy and calibration stability for climate forcing trend detection, as discussed by Wielicki et al. (2013) and Fox et al. (2011). For example, CERES results long measured a TOA +7 W m^{-2} imbalance to the solar energy entering Earth, which is the solar flux arriving at Earth, minus reflected SW and emitted LW. This occurred prior to a one-time "ad hoc" adjustment to the CERES Edition 4.1 SW record's full length by Loeb et al. (2018), to bring the imbalance to a value below +1 W m^{-2}. That was simply because such a value is thought to be realistic by climatologists, but in no way is based on standards traceable calibration from ground or on-orbit [where the term "SI traceable" used later is from Laboratory Accreditation Bureau (2019)].

Perhaps more serious though for climate change studies, was that untracked CERES telescope UV degradation caused the same one-time-adjusted SW results to still falsely drift, because of spurious calibrations trends over time as discussed by Dewitte et al. (2019) and Matthews (2018b, 2021a). To this current date, the most recent CERES SW data are wrongly accepted stable to 0.3 W m^{-2} decade^{-1} by Dessler (2010) and Trenberth et al. (2014) [as originally claimed by NASA at Loeb et al. (2007)]. That makes it measure a false Earth albedo drop that would alone be sufficient to account for up to half of all global warming temperature increases since the year 2000 (Matthews 2021a). The cause of these absolute and stability errors is twofold.

First, the SW absolute calibration of CERES was measured in the ground laboratory using lamps, referenced to a cavity detector called a transfer active cavity radiometer (TACR), also viewing the same lamps and counting photonic energy very accurately. However, the TACR needed to have the same narrow field of view of the laboratory lamps as the CERES device. Therefore, to provide this in prelaunch measurements, a CERES-like Cassegrain silver mirror telescope was installed at the cavity entrance. Unfortunately, the actual TACR mirror telescope reflectivity was never measured at the time, causing analysis to rely on mirror witness samples instead (see Folkman et al. 1994; McCarthy et al. 2011).

Second, CERES optics on-orbit underwent significant contamination and degradation from outgassed particles and

Denotes content that is immediately available upon publication as open access.

Corresponding author: G. Matthews, grant.matthews@zedikasolv.com, grant.matthews@gmail.com

DOI: 10.1175/JTECH-D-21-0002.1

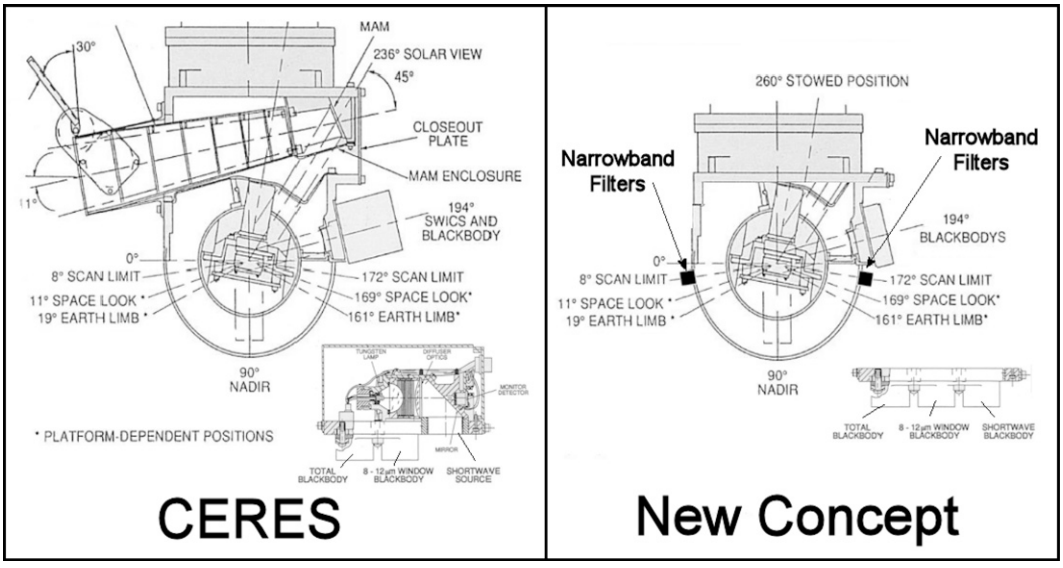

FIG. 1. Comparison of (left) existing CERES (Wielicki et al. 1996) and (right) the new concept design for future improved ERB-type missions.

atomic oxygen exposure, because of the telescope being pointed in the direction of spacecraft travel (see Levine 1992; Matthews et al. 2005, 2006; Matthews 2007, 2009). Such degradation was highly spectrally dependent, with UV changes orders of magnitude greater than in the visible spectral region.

CERES was equipped with solar diffusers called mirror-attenuated mosaics (MAMs) intended for SW calibration, which like the telescopes also spectrally degraded on-orbit, again most heavily in the UV. They were later deemed unusable by Priestley et al. (2011). CERES also had onboard tungsten lamps called the SW internal calibration source (SWICS), but as discussed by Priestley et al. (2000), they also drifted untraceably in output and do not emit UV light of the needed proportions to calibrate an ERB telescope in any case (Loeb et al. 2007). GERB from ESA also has a solar diffuser called a "CalMon," but the constant rapid movement in solar illumination from Geo orbit made its use impractical for the moment (and there is no way to monitor inevitable diffuser degradation, as suffered by CERES). A follow-on from the missions currently existing or in production, therefore, should be designed to better prevent or counter these problems.

2. New low-cost/-risk ERB device calibration design for future missions

a. *Assumptions to overcome deficiencies in existing calibration concepts*

The concept shown here begins with the two discussed assumptions. First, the ground calibration will not transfer to orbit with better than around 1% accuracy because of issues in laboratory procedures, coupled with a possible expected ground contamination event. This contamination event is a worst-case scenario, but actually occurred to the EOS *Aqua* CERES devices between calibration and launch, as mentioned in Matthews et al. (2007a). It then resulted in the Priestley (2006) one-time 8% instrument SW ground-to-flight gain value change to be made, for use in device CFM3's ground processing, with no SI-traceable reason given [remembering that CERES is claimed to be 0.9% absolutely accurate by Wielicki et al. (2013) and Fox et al. (2011)]. Second and as with CERES, outgassing and/or atomic oxygen will put mostly UV absorbing contaminant on the optical mirrors and filters in orbit, continuously degrading their response, with no proven way to track using today's onboard calibration technology.

b. *Proposed alternative solutions*

To save mass and cost, it is recommended to discontinue using solar diffusers and lamps, or other artificial onboard light sources, that have yet to work anywhere near the required accuracy standards. Also, the ERB telescope must maintain the CERES 2005 onward implemented operational constraint, that no telescope can ever face atomic oxygen exposure by pointing the direction of travel (see Matthews et al. 2005; Matthews 2007). Using the design of CERES as a template from the left panel of Fig. 1, this new concept's approximate low-mass and low-cost design is shown on the right panel compared to CERES, without solar diffusers or a lamp for SW calibration. It is, however, important to retain the azimuth rotation capability of CERES, so raster scans of the sun and moon can be performed (facing behind the satellite direction of motion to prevent atomic oxygen exposure). The SWICS lamp should be replaced with a blackbody, slightly warmer than normal, to allow better on-orbit spectral characterization of SW quartz filter thermal leakage, as discussed by Loeb et al. (2001) and Matthews (2018a).

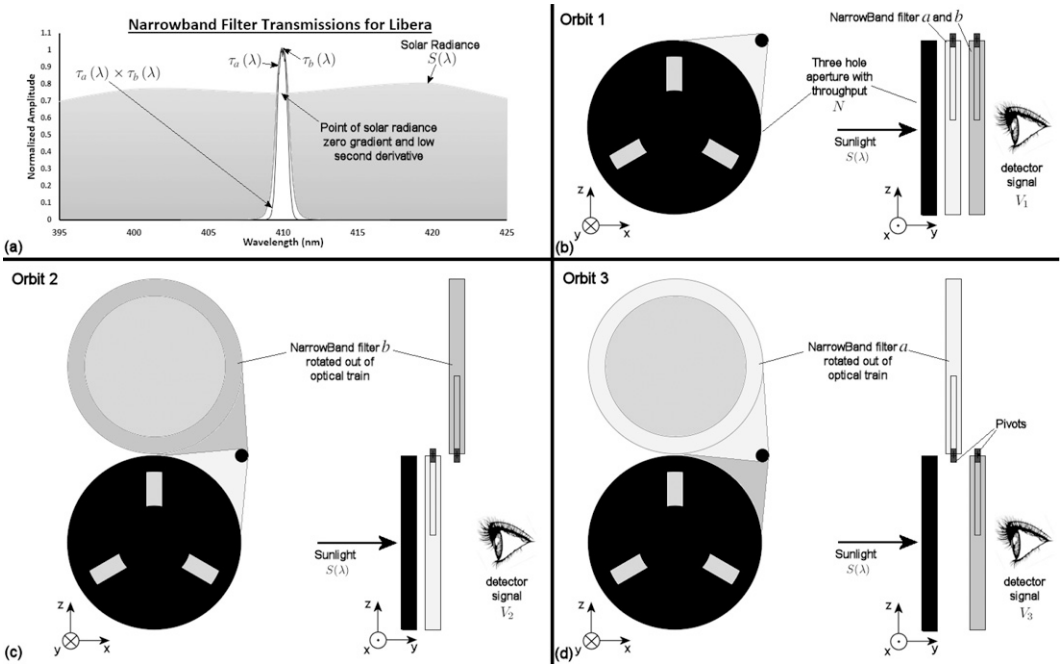

FIG. 2. (a) Narrowband 410-nm-filter FWHM transmissions with 1.5-nm bandwidth. (b) Views sun through compound optic with Cassegrain aperture and two identical narrowband filters each held in or out of optical train with a rotating pivot. (c) As in (b), but with filter *b* removed. (c) As in (b), but with filter *a* removed.

The challenge of using the sun for calibration is that its broadband radiance is around 0.5×10^5 times what a cloud-size-resolution Earth-viewing ERB radiometer can measure without saturating or being damaged, and that dynamic range is beyond current thermal detector technology. For this new concept, narrowband interference filters are installed above the space look on each of the two limb positions as in Fig. 1 (right). Four different pairs of narrowband filters are recommended, of which an example is the 410-nm Alluxa filter shown in Fig. 2a, with a bandwidth approximately 1.5 nm. This will have a ground measured spectral throughput shape $\tau_a(\lambda)$ with a true peak value of around 0.2, meaning a neutral density filter may need to be part of the spectral filter for added attenuation [although the $\tau_a(\lambda)$ and $\tau_b(\lambda)$ functions for use in Eqs. (1), (8), and (10) later will remain normalized to 1 as in Fig. 2a]. Preferably this peak should be at spectral regions covering the UV to the visible, and where the solar spectrum is near to a stationary point, with a low second derivative, to minimize errors from interference filter thermal expansion. Figure 3 makes some rough suggestions for filters to be at around 350, 410, 480, and 650 nm, all with a narrow bandwidth around <2 nm, as it provides greater attenuation and also reduced sensitivity to temperature dependent filter wavelength shifts. All these values remain up for discussion, however. The second near identical filter with spectral transmission shape $\tau_b(\lambda)$ is of course also needed. The Figs. 2b–d

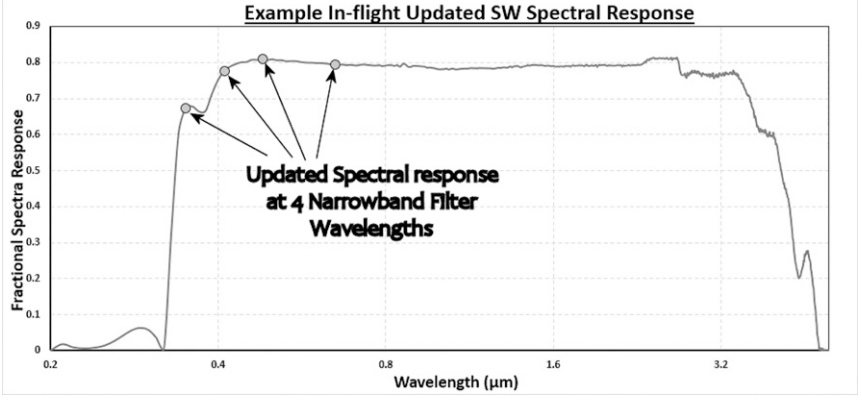

FIG. 3. Example of updated in-flight spectral response.

circular attenuating black metal mask with three holes and around 10% throughput N (measured to <0.1% accuracy on the ground) is required for a further order-of-magnitude signal reduction. This 10% mask should be significantly more accurate and stable than. for example. higher attenuation pinholes or slits, allowing equal illumination of optical surfaces and also reducing diffraction concerns. The solar disk fills an approximate fraction 0.1 of a high-resolution ERB bolometer at the image plane. That allows a rough example calculation using transmission values of each part of the optical train to be given as in Eq. (1) [note this 0.1 fraction of detector area figure used in Eq. (1) is only to demonstrate order of magnitude attenuation]. Remembering that at the mission start peak transmission of filters T_a and T_b are both around 0.2, the needed 2×10^{-5} factor reduction in solar radiance is achieved because solar signal transmission is

$$\text{Calibration Optic Transmission} = 0.1NT_a \frac{\int S(\lambda)\tau_a(\lambda)d\lambda}{\int S(\lambda)d\lambda} \quad (1)$$

$$\approx 2 \times 10^{-5}. \quad (2)$$

The two near identically made narrowband optical filters in the optical train can be rotated in and out of the field of view as in Figs. 2c and 2d with Eq. (2) representing the Fig. 2c case. The normal to the plane of the filter surfaces naturally should not align with that of the telescope, to prevent backscatter affecting the results. The Eq. (3) steradian integral technique of Matthews (2008, 2018a) is to be used on the raw detector signal $v_1(\theta, \phi)$ in Eq. (4), while raster scanning the sun emitting known disk averaged solar spectral radiance $S(\lambda)$ [with n from Eq. (4) the number of the calibration orbit and $\Delta\Omega_{\text{sun}}$ being the steradian angular size of the sun].

SI-traceable calibration is then a three-step, or three-orbit process illustrated in Figs. 2b–d, with the scans performed at only one of the poles to prevent atomic oxygen exposure from the RAM direction, depending on whether in a day-ascending or -descending orbit. During orbit 1 the sun is scanned with both filters in the optical train as in Fig. 2b. With k the wavelength of filter being used, if in the instrument solar spectral response at the peak filter wavelength λ_k is $R_{\lambda k}$ (in V W^{-1} m^{-2} sr^{-1}), then the Eq. (4) integrated result on orbit 1 is represented by Eq. (5):

$$\int d\Omega = \int_0^{2\pi}\int_0^{\pi/2} \sin\theta\, d\theta\, d\phi, \quad (3)$$

$$V_{n,k} = \Delta\Omega_{\text{sun}}^{-1}\int \nu_n(\theta,\phi)d\Omega \quad \text{(volts)}, \quad (4)$$

$$V_{1,k} = R_{\lambda_k}NT_aT_b\int S(\lambda)\tau_a(\lambda)\tau_b(\lambda)d\lambda, \quad (5)$$

$$V_{2,k} = R_{\lambda_k}NT_a\int S(\lambda)\tau_a(\lambda)d\lambda, \quad (6)$$

$$V_{3,k} = R_{\lambda_k}NT_b\int S(\lambda)\tau_b(\lambda)d\lambda. \quad (7)$$

whereas mentioned T_a and T_b are the now unknown peak transmissions of the two filters, at the same wavelength λ_k (e.g., 350, 410, 480, or 650 nm). On the following two orbits, the process is repeated with filter b, then filter a removed from the optical train one at a time, represented by Eqs. (6) and (7) and shown in Figs. 2c and 2d.

Since calibration here is done by scanning on and off celestial bodies, it is important the signal processing use the impulse enhancement (IE) that removes thermal transients in the bolometer signal, since such detectors take time to respond to radiance as described by Matthews (2018c). This will be important because bolometers have various finite time responses and as Fig. 4 shows for an Earth limb scan, other signal processing such as Smith et al. (2002) used by NASA for CERES, will cause a time-constant-dependent bias underestimate of sun and moon mean radiance, while overestimating that of deep space (i.e., the "space clamp" used to remove offsets). Because IE uses three time constants and is tailored to each bolometer as described by Matthews (2018c), it will put all instruments on the same radiance scale for all celestial bodies and remove any remaining space clamp biases that would affect absolute accuracy.

The $S(\lambda)$ mentioned earlier is the known mean SI-traceable solar radiance that is measured by the Total and Spectral Solar Irradiance Sensor mission (TSIS; LASP 2021), monitoring total and spectral output from the sun. The SI-traceable $R_{\lambda k}$ spectral response values at wavelengths λ_k can then be found thus:

$$\alpha_k = \frac{\int S(\lambda)\tau_a(\lambda)d\lambda}{\int S(\lambda)\tau_a(\lambda)\tau_b(\lambda)d\lambda}, \quad (8)$$

$$\beta_k = \int S(\lambda)\tau_b(\lambda)d\lambda \quad \text{(W m}^{-2}\text{ sr)}, \quad (9)$$

$$R_{\lambda_k} = \frac{1}{\alpha_k\beta_k}\frac{V_{2,k}V_{3,k}}{V_{1,k}N} \quad \text{(V W}^{-1}\text{ m}^{-2}\text{ sr}^{-1}\text{)}. \quad (10)$$

The Eq. (8) and (9) constants α and β are calculated from that day's solar spectrum and the accuracy of this technique relies on the spectral shape of the filter throughputs $\tau_a(\lambda)$ and $\tau_b(\lambda)$ not significantly changing, but is independent of their absolute transmission peak magnitudes T_a and T_b (which will undergo inevitable degradation). Finally, the $R_{\lambda k}$ values derived from Eq. (10) can be used to perform monthly spectral updates to the instrument spectral response, as in Fig. 3.

3. Summary and conclusions

Official climate observing system accuracies, such as those on the *Terra*/*Aqua* satellites (NASA 2021), have been assessed as being inadequate for steering and improving climate predictions, of fast-arriving global warming (see Wielicki et al. 2013). The sun is the best calibration target currently in orbit, potentially for viewing and using to correct such on-orbit ERB instrument changes. However, it was mentioned earlier that the difficulty of using it to better calibrate Earth-viewing

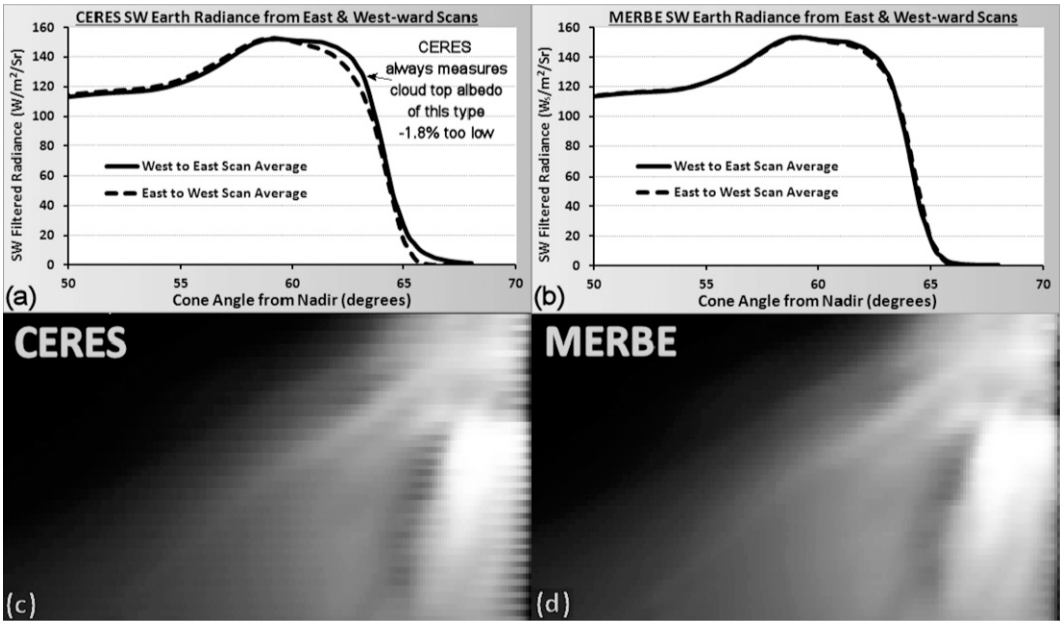

FIG. 4. Comparison of (left) CERES and (right) MERBE east-to-west and west-to-east scans across the Earth limb. (a),(b) Comparison of the raw signals. (c),(d) Comparison of 2D constructed climate results.

radiometers, is that solar radiance is near five orders of magnitude greater than that leaving Earth. With the units of spectral radiance being J s^{-1} m^{-2} μm^{-1} sr^{-1}, most next-generation concepts have concentrated on attenuating the time and space units, by reducing detector integration time in seconds, and great spatial attenuation using pinholes or slits [i.e., reducing seconds, and area in m^2 as in Kopp et al. (2017)]. This proposed concept does not attenuate in space as significantly, or time at all, but instead it does it in wavelength units of μm. That would be the first narrowband ERB concept that uses near direct views of solar radiance by an Earth-viewing telescope, without relying on reflection off a diffusing, hence attenuating, secondary surface (which like all optical components will itself degrade in response). The GERB devices use a mechanism to move the LW rejecting SW quartz filter in and out of the optical train. This means 25 years later, the GERB-like mechanism could be modified to include the narrowband filters of this concept. It should also mean better spectral balancing of the GERB- or CERES-like SW channel with its optical filterless total measuring counterpart, ensuring best accuracy of retrieved daytime LW results [i.e., from the difference in total and SW channel signals; see Matthews et al. (2007b); Matthews (2018b)]. It therefore has the potential to make fully SI-traceable next-generation ERB instruments with both the desired space–time resolution, accuracy, and stability requested by Ohring et al. (2005), Fox et al. (2011), Wielicki et al. (2013), and NRC (2018), making optimal use of all functioning worldly ERB devices.

Recently, it has become the case that calibration stability confidence on the 10^{-1}% $decade^{-1}$ level for data from CERES devices has been actually already achieved using lunar calibration described by Matthews (2008, 2018a), as part of the Moon and Earth Radiation Budget Experiment (MERBE; Matthews 2018b,c, 2021a). This gives an indication that even in the event of this concept's failure, the MERBE stability far superior to that of the higher cost CERES, will still be achieved by such a new device.

However, absolute SI-traceable accuracy of MERBE data from the year 2000 does need to be better achieved and quantified to determine the true value of the "MERBE watt" introduced by Matthews (2018a). As an example then consider that right now it is assumed 1 MERBE watt = 1 true watt, in J s^{-1}. If later it is found lunar albedo is say 1% brighter than thought in creating the Edition 1 MERBE Earth data, it will be the simple case that actually 1 MERBE watt = 1.01 true watts. With the success of this concept measuring the moon as in Matthews (2008, 2018a,c,b), it would then be that lunar-calibrated MERBE Earth data back to the beginning of the century can undergo a one-time adjustment. Such lunar-calibrated MERBE solar data up to 2015 already exist at Matthews (2021c) for free download. So in the example just above, data users can simply apply a 1.01 multiplication of all MERBE SW Earth Edition 1 fluxes from 2000 to 2015 to achieve this. New avenues of improving climate model validation could then be opened, by creating excellent SI-traceable closure of Earth's true radiation budget, dating back to the year 2000.

Acknowledgments. MERBE EBAF-like Ed 1.0 incoming and reflected solar results are downloadable at the FAIR compliant sites (Matthews 2021b,c). CERES instantaneous Edition 1-CV BDS results were obtained from the NASA LaRC Atmospheric Science Data Center.

REFERENCES

Dessler, A. E., 2010: A determination of the cloud feedback from climate variations over the past decade. *Science*, **330**, 1523–1527, https://doi.org/10.1126/science.1192546.

Dewitte, S., N. Clerbaux, and J. Cornelis, 2019: Decadal changes of the reflected solar radiation and the Earth energy imbalance. *Remote Sens.*, **11**, 663, https://doi.org/10.3390/rs11060663.

Folkman, M., and Coauthors, 1994: Calibration of a shortwave reference standard by transfer from a blackbody standard using a cryogenic active cavity radiometer. *1994 IEEE Int. Geoscience and Remote Sensing Symp.*, Pasadena, CA, IEEE, 2298–2300, https://doi.org/10.1109/IGARSS.1994.399719.

Fox, N., A. Kaiser-Weiss, W. Schmutz, K. Thome, D. Young, B. A. Wielicki, R. Winkler, and E. Woolliams, 2011: Accurate radiometry from space: An essential tool for climate studies. *Philos. Trans. Roy. Soc.*, **A369**, 4028–4063, https://doi.org/10.1098/rsta.2011.0246.

Harries, J. E., and Coauthors, 2005: The Geostationary Earth Radiation Budget Project. *Bull. Amer. Meteor. Soc.*, **86**, 945–960, https://doi.org/10.1175/BAMS-86-7-945.

Kopp, G., and Coauthors, 2017: Radiometric flight results from the Hyperspectral Imager for Climate Science (HySICS). *Geosci. Instrum. Methods Data Syst.*, **6**, 169–191, https://doi.org/10.5194/gi-6-169-2017.

Laboratory Accreditation Bureau, 2019: Measurement traceability. LAB, http://www.l-a-b.com/content/measurement-traceability.

LASP, 2021: Solar Radiation and Climate Experiment. Laboratory for Atmospheric and Space Physics, http://lasp.colorado.edu/sorce/.

Levine, A. S., Ed., 1992: LDEF—69 months in space: First post-retrieval symposium, part 3. NASA Conf. Publ. 3134, 488 pp., https://sites.google.com/site/zedikasolv/LDEFresults.pdf?attredirects=0&d=1.

Loeb, N. G., K. J. Priestley, D. P. Kratz, E. B. Geier, R. N. Green, and B. A. Wielicki, 2001: Determination of unfiltered radiances from the Clouds and the Earth's Radiant Energy System instrument. *J. Appl. Meteor.*, **40**, 822–835, https://doi.org/10.1175/1520-0450(2001)040<0822:DOURFT>2.0.CO;2.

——, and Coauthors, 2007: Multi-instrument comparison of top-of-atmosphere reflected solar radiation. *J. Climate*, **20**, 575–591, https://doi.org/10.1175/JCLI4018.1.

——, and Coauthors, 2018: Clouds and the Earths Radiant Energy System (CERES) Energy Balanced and Filled (EBAF) top-of-atmosphere (TOA) Edition-4.0 data product. *J. Climate*, **31**, 895–918, https://doi.org/10.1175/JCLI-D-17-0208.1.

Matthews, G., 2007: Animation of CERES contamination mobilization and polymerization mechanism. Google, https://sites.google.com/site/zedikamerbe/CERESContamination.wmv?attredirects=0&d=1.

——, 2008: Celestial body irradiance determination from an under-filled satellite radiometer: Application to albedo and thermal emission measurements of the moon using CERES. *Appl. Opt.*, **47**, 4981–4993, https://doi.org/10.1364/AO.47.004981.

——, 2009: In-flight spectral characterization and calibration stability estimates for the Clouds and the Earth's Radiant Energy System (CERES). *J. Atmos. Oceanic Technol.*, **26**, 1685–1716, https://doi.org/10.1175/2009JTECHA1243.1.

——, 2018a: First decadal lunar results from the Moon and Earth Radiation Budget Experiment (MERBE). *Appl. Opt.*, **57**, 1594–1610, https://doi.org/10.1364/AO.57.001594.

——, 2018b: Real-time determination of Earth radiation budget spectral signatures for nonlinear unfiltering of results from MERBE. *J. Appl. Meteor. Climatol.*, **57**, 273–294, https://doi.org/10.1175/JAMC-D-16-0406.1.

——, 2018c: Signal processing enhancements to improve instantaneous accuracy of a scanning bolometer: Application to MERBE. *IEEE Trans. Geosci. Remote Sens.*, **56**, 3421–3431, https://doi.org/10.1109/TGRS.2018.2799823.

——, 2021a: Nasa CERES spurious calibration drifts corrected by lunar scans to show the sun is not increasing global warming and allow immediate CRF detection. *Geophys. Res. Lett.*, **48**, e2021GL092994, https://doi.org/10.1029/2021GL092994.

——, 2021b: MERBE ed1.0 incoming solar data download. Pangaea, accessed 19 March 2022, https://doi.org/10.1594/PANGAEA.931778.

——, 2021c: MERBE ed1.0 reflected solar data download. Pangaea, accessed 19 March 2022, https://doi.org/10.1594/PANGAEA.931779.

——, K. Priestley, P. Spence, D. Cooper, and D. Walikainen, 2005: Compensation for spectral darkening of short wave optics occurring on the Cloud's and the Earth's Radiant Energy System. *Proc. SPIE*, **5882**, 354–365, https://doi.org/10.1117/12.618972.

——, ——, N. G. Loeb, K. Loukachine, S. Thomas, D. Walikainen, and B. A. Wielicki, 2006: Coloration determination of spectral darkening occurring on a broadband Earth observing radiometer: Application to Clouds and the Earth's Radiant Energy System (CERES). *Proc. SPIE*, **6296**, 62960M, https://doi.org/10.1117/12.680884.

——, ——, and S. Thomas, 2007a: Transfer of radiometric standards between multiple low Earth orbit climate observing broadband radiometers: Application to CERES. *Proc. SPIE*, **6677**, 66770I, https://doi.org/10.1117/12.734478.

——, ——, and ——, 2007b: Spectral balancing of a broadband Earth observing radiometer with co-aligned short wave channel to ensure accuracy and stability of broadband daytime outgoing long-wave radiance measurements: Application to CERES. *Proc. SPIE*, **6678**, 66781H, https://doi.org/10.1117/12.734492.

McCarthy, J. K., H. Bitting, T. A. Evert, and M. E. Frink, 2011: Performance and long-term stability of the prelaunch radiometric calibration facility for the Clouds and the Earth's Radiant Energy System instruments. *IEEE Trans. Geosci. Remote Sens.*, **51**, 684–694, https://doi.org/10.1109/TGRS.2012.2195726.

NASA, 2021: Earth Observing System Terra, Aqua and NPP. NASA, https://eospso.nasa.gov/current-missions.

NRC, 2018: *Thriving on Our Changing Planet: A Decadal Strategy for Earth Observation from Space.* National Academies of Science, 716 pp., https://www.nap.edu/catalog/24938/thriving-on-our-changing-planet-a-decadal-strategy-for-earth.

Ohring, G., B. A. Wielicki, R. Spencer, B. Emery, and R. Datla, 2005: Satellite instrument calibration for measuring global climate change. *Bull. Amer. Meteor. Soc.*, **86**, 1303–1314, https://doi.org/10.1175/BAMS-86-9-1303.

Priestley, K. J., 2006: Nasa CERES website of production gain changes to AV values. Google, https://sites.google.com/site/cerescalarchive/CERESproductiongains.pdf?attredirects=0&d=1.

——, and Coauthors, 2000: Postlaunch radiometric validation of the Clouds and the Earth's Radiant Energy System (CERES) proto-flight model on the Tropical Rainfall Measuring Mission (TRMM) spacecraft through 1999. *J. Appl. Meteor.*, **39**, 2249–2258, https://doi.org/10.1175/1520-0450(2001)040<2249:PRVOTC>2.0.CO;2.

——, and Coauthors, 2011: Radiometric performance of the CERES Earth radiation budget climate record sensors on the EOS *Aqua* and *Terra* spacecraft through April 2007. *J. Atmos. Oceanic Technol.*, **28**, 3–21, https://doi.org/10.1175/2010JTECHA1521.1.

Smith, G. L., D. K. Pandey, R. B. Lee, B. R. Barkstrom, and K. J. Priestley, 2002: Numerical filtering of spurious transients in a satellite scanning radiometer: Application to CERES. *J. Atmos. Oceanic Technol.*, **19**, 172–182, https://doi.org/10.1175/1520-0426(2002)019<0172:NFOSTI>2.0.CO;2.

Trenberth, K. E., J. T. Fasullo, and M. A. Balmaseda, 2014: Earth's energy imbalance. *J. Climate*, **27**, 3129–3144, https://doi.org/10.1175/JCLI-D-13-00294.1.

Wielicki, B. A., B. R. Barkstrom, E. F. Harrison, R. B. Lee, G. L. Smith, and J. E. Cooper, 1996: Clouds and the Earth's Radiant Energy System (CERES): An Earth observing experiment. *Bull. Amer. Meteor. Soc.*, **77**, 853–868, https://doi.org/10.1175/1520-0477(1996)077<0853:CATERE>2.0.CO;2.

——, and Coauthors, 2013: Achieving climate change absolute accuracy in orbit. *Bull. Amer. Meteor. Soc.*, **94**, 1519–1539, https://doi.org/10.1175/BAMS-D-12-00149.1.